A curvilinear Model Approach: Actin Cortex Clustering Due to ATP-induced Myosin Pulls

Christian Wölfer * **Sven K. Vogel** ** **Michael Mangold** *

* *Max Planck Institute for Dynamics of Complex Technical Systems, 39106 Magdeburg, Germany*
** *Max Planck Institute of Biochemistry, 82152 Martiensried, Germany*

Abstract: The actomyosin cortex is involved in a range of many cellular processes like cell division, motility or shaping. To obtain this variety of functionalities the membrane-bound actin mesh has to be reconstituted by the motor protein myosin. But little is known about the underlying mechanism, which control the different tasks. An underlying in vitro study of a synthetic actomyosin cortex has shown that the cortex organizes into spatial clusters for certain ATP concentrations. Here we develop a curvilinear model that captures the viscoelastic material behavior and the kinetics of the myosin cross bridge. Further, we suggest a formulation for the active contractile stress produced by the motor protein myosin. We demonstrate that the spatial pattern generated by the curvilinear model is consistent with the experimental observations, including mesh clustering due to contractile forces and an absence of contraction for low and high ATP concentrations. Additionally we show that the cluster positioning can be tuned by the ATP-gradient.

Keywords: Actin-Myosin Cortex, Dynamic Modeling, Distributed Model, System Analysis, Synthetic Biology

1. INTRODUCTION

The cell cortex formed by actin filaments is an important functional unit of almost all eucaryotic cells. As one of the three cytoskeleton components actin is involved in a variety of basic cellular processes such as cell division, motility, formation and stabilization of cell shape, or exocytosis and endocytosis (Theriot et al., 2002). Therefore it is a very interesting system for the bottom-up synthetic biology, which pursues the goal of creating minimal cell-imitating entities from non-living biological components such as lipids, proteins and DNA (Schwille, 2011).

1.1 The Actomyosin Cortex

The monomer globular G-actin polymerizes, both spontaneously and regulated by a variety of factors, to filamentous F-actin which forms a meshlike structure via crosslinker proteins like Arp 2/3 or Filamin (Stossel et al., 2001). Membrane anchors interlink the inner plasma membrane with the F-actin and create a region of high F-actin density close to the membrane in the so-called cell cortex. Due to the additionally occurring depolymerization of F-actin the whole network is a very dynamic structure, which is jointly responsible for some of the key functions of actin. The mesh-like structure causes the viscoelastic or gel-like material behavior of the F-actin, and thereby, combines the characteristics of a fluid and solid, which is closely connected to the generated forces by the network (Claessens et al., 2006). In addition to these internal

forces, the motor protein myosin II contracts the meshwork through consumption of chemical energy provided by the cellular energy storage molecule ATP and converting it into mechanical energy. Myosin II is a complex filamentous protein (myofilament) with a variety of myosin heads, also known as motor domain, on both opposite sides of the protein, and a head-free neck domain in between. The underlying myosin cross bridge cycle for a myosin head (Rayment et al., 1993) is a well known and well described biochemical circuit (Fig. 1A). In a simplified consideration the circuit can be described by four main reaction steps. The first step (r_1) is a hydroxylation of ATP to ADP which is linked to an myosin head (M) . This hydroxylation step
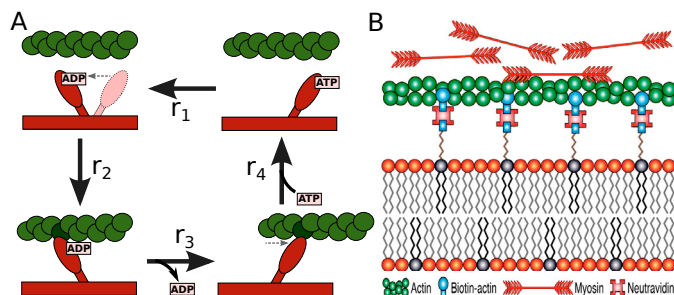

Fig. 1. (A)Biochemical myosin cross bridge cycle of a motor domain which is responsible for the conversion of chemical into mechanical energy. (B) Scheme of a minimal actin cortex MAC (Vogel et al., 2013)

provides the energy for a conformational change of the myosin head into the active state (M'). In the active state the myosin head is able to interact with the F-actin (r_2) and to form an active actomyosin complex (A-M').

The unstable active actomyosin complex is converted very fast into the inactive state (A-M) by releasing the bound ADP (r_3). In addition, the ADP dissociation causes a further spatial conformational change of the myosin head and, because of the mechanical coupling, an acceleration of the F-actin filament. Considering that motor domains on both sides of myosin can interact with F-actin, the acceleration or power stroke of myosin heads could result in a buckling, breakage and compaction of a F-actin filament and finally due to cross connections in a contraction of the meshwork.

1.2 Experimental Motivation for this work

To investigate the actin cortex in experiments in vitro under cell-free and thus noise-free conditions, 'minimal actin cortices' (MACs: Fig. 1B) were developed consisting of biotinylated F-actin filaments which are connected to a lipid bilayer via neutravidin linkers, myosin II motor proteins and enzymatically regenerated ATP (Vogel and Schwille, 2012). Experiments with MACs suggest that myosin contraction of the actin cortex causes initially some small F-actin clusters that merge to larger ones after a certain time (Fig. 2). In addition, the investigation of the ATP dependency of F-actin clustering revealed that no clustering occurs for a very low ATP level corresponding to a too low energy level (Vogel et al., 2013). Surprisingly, no contractions were observable either for higher ATP concentrations (Table 1). Thus pattern formations occur only for medium ATP concentrations, which could be a cellular control mechanism for actin cortex.

How the different functions and patterns of the actin cortex, like network reorganization while cell division, are cellularly regulated is poorly understood, despite a large number of in vivo and in vitro experiments. However it is very likely that the active contractions of the motor protein myosin under ATP consumptions play a key role in controlling pattern formations in the actin cortex.

1.3 Objective of this work

Mathematical models support the experiments by providing insight into the system dynamics and unmeasurable states. Thus it is the aim of this work to develop a mathematical model, which reproduces the experimental observations and help to understand the pattern formation in the actin cortex. The model is based on previous work in literature (Lewis et al., 2014; George et al., 2013). As a new aspect of our model, compared to published work, the dependence of cluster formation on ATP is described by including the biochemical myosin bridge circuit in a spatially distributed model.

2. MODEL

In the following, a mathematical model is presented whose purpose is to explain the experiment findings in a qualitative manner. A two dimensional continuum model in polar coordinates has been developed as a cut through a spherical cell. For modeling the cortex it is assumed that the

Table 1. ATP dependency of myosin contraction (0,3 μM myosin II) with enzymatically regenerated ATP. Contractions are meant as qualitatively visible rearrangement or clustering of MACs after myosin addition at a certain ATP level (Vogel et al., 2013).

Regenerated ATP concentration [μM]	Contraction
12.5	No
10	No
1	Yes
0.3	Yes
0.1	Yes
0	No

actomyosin species are located close to the inner site of the membrane in a very thin layer. Therefore it can be assumed that the actomyosin cortex does not change radially and has a fixed radius which is scaled to $R_0 = 1$. This results in a one dimensional ring geometry with periodic boundary conditions for the actomyosin species. In contrast, ATP diffuses through the whole two dimensional system and is only consumed by the membrane linked actomyosin cortex. For simplifying the model formulation, it is assumed that the forces generated by the surrounding medium (containing monomer G-actin) are negligible. Thus a one phase model is sufficient to describe the forces in the actin cortex. The balance of momentum density J as a product of F-actin density A scaled by a density parameter ϱ_A and a velocity V ($J = \varrho_A \cdot A \cdot V$) is expressed as

$$\frac{\partial J}{\partial t} + \frac{\partial J \cdot V}{\partial \varphi} = \frac{\partial}{\partial \varphi}(\sigma_V - \sigma_e + \sigma_m), \quad (1)$$

with the angular component φ in a range of $[0, 2\pi]$. The left-hand side of the equation represents the material derivative of the momentum density which can be interpreted as the convective flux of momentum due to F-actin flow V. The terms on the right-hand side constitute the acting forces of the system. The first term models the viscous stress or shear stress

$$\sigma_V = \eta \frac{\partial V}{\partial \varphi}, \quad (2)$$

which is generated by F-actin filaments moving relative to each other . It is the one dimensional representation of the stress tensor $\tau_{\varphi\varphi}$ with viscosity parameter η (Bird et al.,
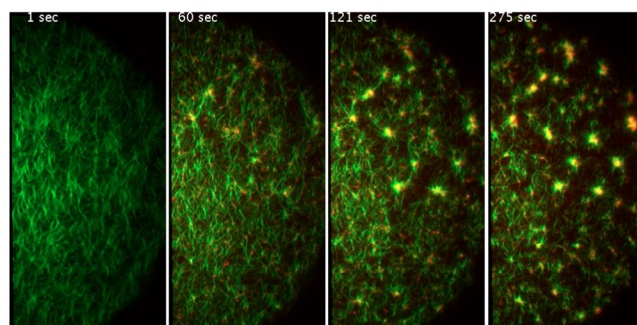

Fig. 2. Clustering of green labeled actin meshwork after addition of red labeled myosin II and ATP from Vogel et al. (2013).

1960). Because of the one dimensional model geometry, the viscosity parameter could be understood as a sum of the dynamic and the bulk viscosity coefficient. For representing the whole viscoelastic material behavior, the second term describes the stress generated by relaxation of network deformation e:

$$\sigma_e = G(e - 1). \tag{3}$$

The term for elastic stress used here was firstly derived by Lewis et al. (2014). The elastic modulus G is assumed as super-linear scaled with the F-actin density

$$G = g \cdot A_{tot}^q, \tag{4}$$

with a scaling parameter $q = 2.2$ according to in vitro measurements of the viscoelastic behavior of F-actin (MacKintosh et al., 1995). As a new idea, the myosin power stroke is modeled by the mass action reaction rate r_3, which is responsible for the acceleration of F-actin filaments (Fig. 1A), times the concentration of inactive actomyosin (A-M):

$$\sigma_m = max[0, p \cdot r_3 \cdot A\text{-}M - f_{min}]. \tag{5}$$

The fundamental idea is that the myosin can only bend, break and compact a filament when both sides of the myofilament are connected to the F-actin mesh. Otherwise the power stroke would not be transmitted sufficiently and instead would move the motor protein along the filament. The more myosin heads are bound to the F-actin filament, the better should the transmission of power stroke be. Thus in our formulation the transmitted power stroke is scaled by the concentration of inactive actomyosin and the parameter p. In addition, the active stress has to exceed a certain minimal force f_{min}, which is motivated by the overcoming of the F-actin bending force and the breakage of certain membrane anchors (Howard, 2001). The formulation with a maximum function is used to prevent a negative power stroke or rather a elongation of the actin filaments for low ATP concentrations.

The partial differential equation for the volumetric network strain e, derived by Lewis et al. (2014), is given as

$$\frac{\partial e}{\partial t} + \frac{\partial(e \cdot V)}{\partial \varphi} = \lambda(1 - e). \tag{6}$$

The equation contains the transport of local network strain together with the F-actin mesh and the relaxation of strain, where $e = 1$ represents the unstrained state and $e > 1$ the network compression with the relaxation rate λ. The evolution of F-actin A obeys an advection-diffusion equation with additional mass action reaction rates:

$$\frac{\partial A}{\partial t} + \frac{\partial(A \cdot V)}{\partial \varphi} = D_A \frac{\partial^2 A}{\partial \varphi^2} - r_2 + r_4. \tag{7}$$

In contrast to other published models (Jülicher et al., 2007; Ramaswamy and Jülicher, 2016) polymerization, depolymerization and, as a consequence, polarity of F-actin filaments are not taken into account because of the insignificant role in the in vitro experiments.

The following partial different equations constitute the spatially distributed myosin cross bridge model. The actomyosin species A-M and A-M', which are transported together with the mesh, are modeled by advection-diffusion equations with the associated reaction rates (10,11). In contrast, the unbound myosin species (M and M') are represented by simpler diffusion equations and mass action reaction rates (8,9).

$$\frac{\partial M}{\partial t} = D_M \frac{\partial^2 M}{\partial \varphi^2} + r_4 - r_1, \tag{8}$$

$$\frac{\partial M'}{\partial t} = D_M \frac{\partial^2 M'}{\partial \varphi^2} + r_1 - r_2, \tag{9}$$

$$\frac{\partial A\text{-}M'}{\partial t} + \frac{\partial(A\text{-}M' \cdot V)}{\partial \varphi} = D_A \frac{\partial^2 A\text{-}M'}{\partial \varphi^2} + r_2 - r_3, \tag{10}$$

$$\frac{\partial A\text{-}M}{\partial t} + \frac{\partial(A\text{-}M \cdot V)}{\partial \varphi} = D_A \frac{\partial^2 A\text{-}M}{\partial \varphi^2} + r_3 - r_4. \tag{11}$$

For simplicity and to keep a cortex like structure the diffusion in (7-11) are limited to the angular direction. Because ATP is able to diffuse through the whole system, the partial differential equation of ATP contains diffusion in angular and additional radial direction, and the reaction rate r_4, in which ATP is consumed:

$$\frac{\partial ATP}{\partial t} = D_{ATP} \left(\frac{1}{R} \frac{\partial}{\partial R} \left(R \frac{\partial ATP}{\partial R} \right) + \frac{1}{R^2} \frac{\partial^2 ATP}{\partial \varphi^2} \right), \tag{12}$$

with the radial boundary condition:

$$D_{ATP} \frac{\partial ATP}{\partial R} | R_0, \varphi = r_4, \tag{13}$$

and periodic boundary conditions in angular direction. To improve the numerical solution and analysis of simulation, a nondimensionalization is performed with the droplet radius R_0, the strain relaxation time λ and viscosity parameter η as characteristic scaling parameters (Table 2). Furthermore the concentrations of actomyosin species should be understood as scaled concentrations which are defined as:

$$A = a/a_0, \qquad ATP = atp/atp_0,$$
$$M' = m'/m'_0, \qquad M = m/m_0,$$
$$A\text{-}M = a\text{-}m/a\text{-}m_0, \qquad A\text{-}M' = a\text{-}m'/a\text{-}m'_0,$$
$$\tilde{J} = \frac{J \cdot R_0}{\eta}, \qquad \tilde{V} = \frac{J}{\varrho_A \cdot A \cdot \lambda \cdot R_0}.$$

The equations 1-12 represent a coupled, nonlinear system of partial differential equations. It is discretized with a finite volume method and an upstream scheme.

3. RESULTS

The modeling and simulations are performed with the software packages Promot and Diana (Krasnyk et al., 2006), after a spatial discretization with finite volume method. The parameters 2 are adjusted accordingly to reproduce the experimental observations, whereby the scaling parameter for elastic stress α is taken from Lewis et al.

Table 2. Nondimensionalized system parameters with chosen parameter values.

Parameter	Definition	Parameter Value
α	$\frac{g}{\lambda \cdot \eta}$	0.1
ψ	$\frac{p}{\lambda \cdot \eta}$	5.0
F_{min}	$\frac{f_{min}}{\lambda \cdot \eta}$	0.01
$\tilde{D}_A$	$\frac{D_A}{\lambda}$	10^{-5}
$\tilde{D}_M$	$\frac{D_M}{\lambda}$	10^{-4}
$\tilde{D}_{ATP}$	$\frac{D_{ATP}}{\lambda}$	$5 \cdot 10^{-3}$

(2014). Moreover, the diffusion parameters are chosen so that the different mass diffusivities of polymeric actin and free-moving ATP and myosin molecules are taken into account. The initial concentration of the scaled F-actin density is set to 1 and the scaled myosin concentration to an average value of 0.5, representing a dense actomyosin mesh (Vogel et al., 2013). To disturb the system initially, the concentration of active unbound myosin (M') is given as a very small periodic distribution (fluctuations of 0.01 around the average) to obtain a variety of clusters. All other concentrations are considered to be homogeneous and in an unstrained state.

To investigate the influence of ATP on F-actin cortex clustering, simulations have been conducted with diverse ATP initial concentrations. It has been found that different ATP initial concentrations generate different patterns of cortex clustering. When setting the scaled ATP concentration to
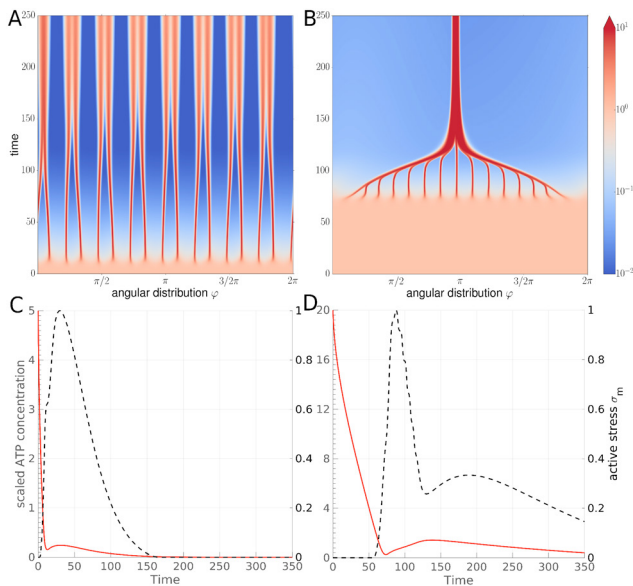
Fig. 3. Transient model dynamics of the scaled F-actin density A (shown by color bar) with the standard parameter set (table 2). A: Absence of total clustering of F-actin mesh with an initial value of 5 for scaled ATP concentration. B: Clustering of F-actin mesh with a starting value of scaled ATP concentration of 20. C: Time evolution of average scaled ATP concentration (red line) and average active contractile stress (black dashed) for initially 5 and, D: 20 units of scaled ATP concentration.
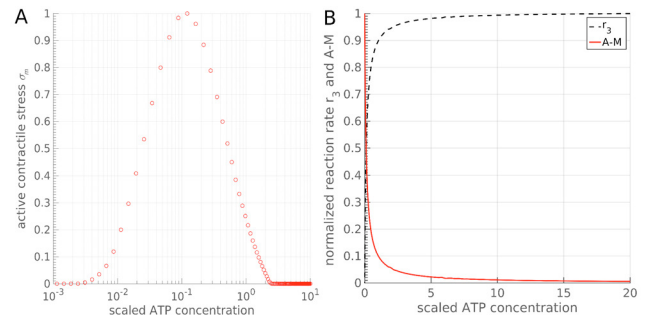
Fig. 4. A: Dose-response curve of the normalized average active contractile stress in the cortex region ($R = R_0$) in dependency to the average of ATP concentration in a logarithmic scale. B: Dose-response curve of normalized average of reaction kinetic r_3 (A.3), responsible for power stroke, and normalized concentration of inactive actomyosin A-M, responsible for stroke transmission, in dependency to the average of scaled ATP concentration, as components of contractile active stress σ_m.

5 units (Fig. 3A), local actin clusters form very fast after 5 time steps, while attracting each other (identifiable by high density spots moving against each other) till time step 150. After time point 150 the cluster attraction stops and only diffusion is acting on the network, visible by a blurring of the clusters in Fig. 3A. ATP streams continuously from the bulk region of the system into the cortex and is consumed there by the releasing reaction of inactive myosin heads in reaction rate r_4. The absence of clustering is according to a drop of ATP concentration, under a certain threshold, which prevents active contraction (Fig. 3C). In contrast, when beginning initiating with a scaled ATP concentration of 20 units, the actin mesh remains homogeneous till around time point 75. Afterwards clustering occurs with a global merging of all local clusters to one dense F-actin cluster (Fig. 3B). The clusters do not form before the ATP concentration in the cortex has dropped under a certain threshold. After the mering to one F-actin cluster, ATP is still present in the system up to the end of simulation time (Fig. 3D). This keeps the system in a kind of steady state, where ATP constantly streams in by diffusion from the bulk region and causes a permanent network contraction, which is balanced by viscous and especially elastic stress (strain relaxation), preventing the mesh from contracting to a non-physical infinitely dense cluster.

The mentioned ATP-thresholds for loss of network contraction are represented in the dose-response curve for the used parameter set (table 2), which illustrates the dependency of active contractile stress on the ATP concentration (Fig. 4A). This dependency correlates very well with the experimental observed occurrence of cluster formations at medium ATP concentrations (table 1). This desired system behavior is caused by the formulation for the active contractile stress σ_m (5). The underlying idea for this formulation is discussed in the following. The power stroke performed by a myosin head is subject to a loss of force transmission on the mesh for higher ATP concentrations and a loss of energy supply for lower ATP concentration. In Fig. 4B this aspect is clarified. For high ATP concentrations the generated force is high as well, and reaches a steady state for further increasing ATP concentration

because of saturation of the myosin cross bridge model. So further increasing of the ATP concentration would have no effect on the reaction rate r_3 or the pure power stroke performed by a myosin head. In contrast, the concentration of inactive actomyosin (A-M), which connects of the pulling myosin head with the actin filament, is very low. Because of the high ATP concentration myosin heads are released fast from the actin filament, so that in average nearly no inactive myosin head is bound long enough to bend, break and compact a filament. The myosin power stroke in the case of high ATP concentration results in a movement of the myosin molecule along the actin filament with a maximal velocity due to saturation of myosin cross bridge cycle. A decreasing ATP concentration results in a increasing concentration of inactive actomyosin heads, which improves the force transmission. But it results in a decreasing of generated force by reaction rate r_3 as well. Hence, the active stress reaches a maximum, in fig. 4A around 0.01 ATP concentration, and decreases afterwards with decreasing ATP concentration. For very low ATP concentrations nearly all myosin heads stay in the rigor-like inactive actomyosin state and cut off the myosin cross bridge cycle.

Finally, the influence of the spatial ATP-gradient on the formation of clusters is investigated. To this purpose, the used parameter set (table 2) is changed slightly by setting the scaling parameter for elastic stress, so called elastic resistance (Lewis et al., 2014), to $\alpha = 0.01$ and the minimal force, which adapts the width of the dose-response curve, to $F_{min} = 0.02$. A simulation with this changed parameter set and an initial concentration of 10 units scaled ATP concentration reveals a clustering to just two main F-actin clusters opposite to each other in the ring topology (Fig 6A). Because of the reduced elastic resistance, the merging to a few main clusters is now less inhibited and no local clusters are present, in contrast to Fig. 3. Further investigations with the elastic resistance reveal that for high values of $\alpha > 1$ only local clusters are observable, which do not converge to one main cluster (Fig. 5). Due to increasing minimal force the contraction stops earlier than in the previous case ($T = 60$), resulting in a blurring of the F-actin clusters due to diffusion. To investigate the influence of the ATP-gradient, an additional influx of 10 units scaled ATP concentration from time point 100 to 150 is assumed and simulated at different angular positions in the cortex. An ATP influx at the angular position $\varphi = \pi$ constitutes a new ATP-gradient and results in a further attraction of the two opposite clusters, which merge to one main cluster at angular position $\varphi = \pi$ (fig. 6B). The influx at the opposite site ($\varphi = 2\pi$) also results in a main cluster formation at the influx position (fig. 6C). The simulation results suggest that ATP gradients are potentially jointly responsible for occurrence and the positioning of clustering in the cell cortex.

4. DISCUSSION

The F-actin cortex is involved in many main cellular processes. Possibly due to this variety of tasks the network is a very complex material whose control mechanism are mainly unknown. The aim of this work is to generate a simplified model of an actin cortex, which regenerates the experimental observations of clustering of an in-vitro MAC for certain ATP concentrations. The simulation results
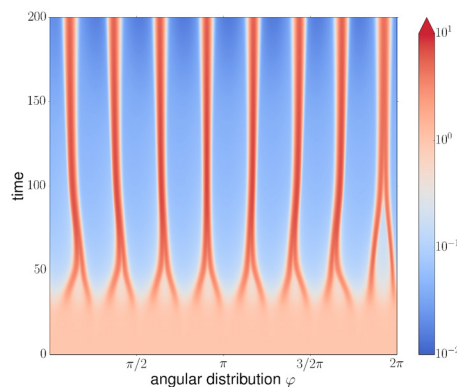

Fig. 5. Absence of network clustering for $\alpha = 1$ with parameter set (table 2).

show that the model is able to cluster a homogeneous F-actin density to one main cluster or a variety of clusters because of a new formulation for the active contractile stress, which models the dependency of cluster formation on a medium ATP concentration. The simulation results further suggest, that cluster formation is only obtained when active contraction and a viscoelastic material behavior are present (Fig. 3B). The formulation of the active stress bases on the species of the well described myosin cross bridge model (Rayment et al., 1993; Howard, 2001). In addition in vitro studies, which observed a movement of myosin proteins along actin fibers, support our new formulation of active contractile stress (Sheetz and Spudich, 1983; Vogel et al., 2013). The tendency of merging of various local clusters to one main cluster is owed to the continuity model structure, which models no empty space, with the consequence that everything is connected and can attract each other. In the underlying in vitro experiment the F-actin mesh contracts to a variety of clusters where the actin density in between very is low or empty room is present so that the generated forces are too small to merge all cluster. Thus the presence of a variety of cluster correlate not necessarily with a depletion of ATP like in Fig. 3A.

Furthermore our results suggest, that ATP may be involved in cellular control of occurrence and positioning of F-actin cluster by creating a local ATP gradient, which is followed by the merging clusters. Network contraction in different regions is necessary for amoeba-like crawling cells. In the front region of these cells the network polymerization is predominant to protrude the membrane, and network contraction dominates in the rear region to pull the cell bulk after (Mogilner, 2009). An ATP-gradient with a high concentration in the front region, which accelerates the network polymerization, and a medium concentration in the rear region, which enables myosin contraction, could be a pattern which generates cell motility.

Since it was the objective of the model to describe the clustering induced by myosin power strokes, the chosen curvilinear respectively ring topology was sufficiently detailed.
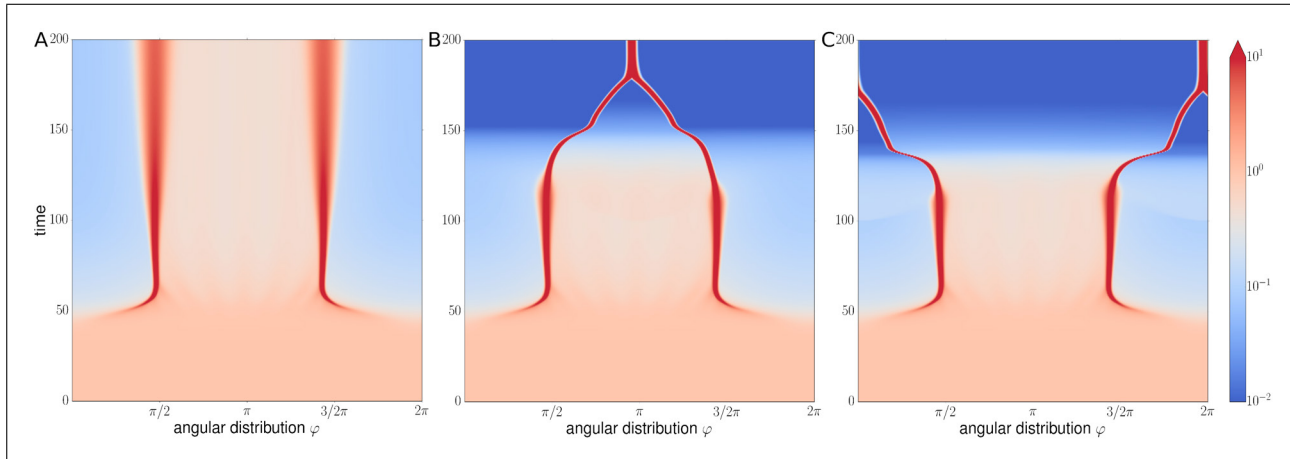
ACKNOWLEDGEMENTS

Fig. 6. Transient model dynamic of the scaled F-actin density A with changed parameter values for $\alpha = 0.01$ and $F_{min} = 0.02$ in comparison to the values in table 2 and initially 20 units scaled ATP concentration. A: Stop of Clustering of two F-actin clusters after ATP depletion. B: Clustering of two F-actin clusters after feeding of 10 units scaled ATP concentration at angular coordinate of $\varphi = \pi$. C: Clustering of F-actin mesh after ATP feed at angular position $\varphi = \pi/2$.

REFERENCES

Bird, R.B., Stewart, W.E., and Lightfoot, E.N. (1960). *Transport Phenomena*. John Wiley and Sons.

Claessens, M.M.A.E., Tharmann, R., Kroy, K., and Bausch, A.R. (2006). Microstructure and viscoelasticity of confined semiflexible polymer networks. *Nature Physics*, 2, 186–189.

George, U.Z., Stephanou, A., and Madzvamuse, A. (2013). Microstructure and viscoelasticity of confined semiflexible polymer networks. *Mathematical Biology*, 66, 547–593.

Howard, J. (2001). *Mechanics of Motor Proteins and the Cytoskeleton*. Sunderland, MA: Sinauer.

Jülicher, F., Kruse, K., Prost, J., and Joanny, J.F. (2007). Active behavior of the cytoskeleton. *Physics Reports*, 449, 3–28.

Krasnyk, M., Bondareva, K., Milokhov, O., Teplinskiy, K., Ginkel, M., and Kienke, A. (2006). The promot/diana simulation environment. *Computer Aided Chemical Engineering*, 21, 445–450.

Lewis, O.L., Guy, R.G., and Allard, J.F. (2014). Actin-myosin spatial patterns from a simplified isotropic viscoelastic model. *Biophysical journal*, 107, 863–870.

MacKintosh, F.C., Käs, J., and Janmey, P. (1995). Elasticity of semiflexible biopolymer networks. *Physical Review Letters*, 75, 4425–4428.

Mogilner, A. (2009). Mathematics of cell motility: have we got its number? *Journal of mathematical biology*, 58, 105–134.

Ramaswamy, R. and Jülicher, F. (2016). Activity induces traveling waves, vortices and spatiotemporal chaos in a model actomyosin layer. *Scientific Reports 6*.

Rayment, I., Holden, H.M., Whittaker, M., Yohn, C.B., Lorenz, M., Holmes, K.C., and Milligan, R.A. (1993). Structure of the actin-myosin complex and its implications for muscle contraction. *Science*, 261, 58–65.

Schwille, P. (2011). Bottom-up synthetic biology: Engineering in a tinkerers world. *Science*, 333, 1252–1254.

Sheetz, M.P. and Spudich, J.A. (1983). Movement of myosin-coated fluorescent beads on actin cables in vitro. *Nature*, 303, 31–35.

Stossel, T.P., Condeelis, J., Cooley, L., Hartwig, J.H., Noegel, A., Schleicher, M., and Shapiro, S.S. (2001). Filamins as integrators of cell mechanics and signalling. *Nature Reviews Molecular Cell Biology*, 2, 138–145.

Theriot, J., Amos, L., Cooper, J., Fuchs, E., Gertler, F., Goldstein, L., Howard, J., Machesky, L., McNally, F., Mitchison, T., and Solomon, F. (2002). The cytoskeleton. In B. Alberts, A. Johnson, J. Lewis, M. Raff, K. Roberts, and P. Walter (eds.), *Molecular Biology of the Cell*, 889–963. Garland Science.

Vogel, S.K., Petrasek, Z., Heinemann, F., and Schwille, P. (2013). Myosin motors fragment and compact membrane-bound actin filaments. *Cytoskeleton (Hoboken)*, 70, 706–717.

Vogel, S.K. and Schwille, P. (2012). Minimal systems to study membrane-cytoskeleton interactions. *Curr Opin Biotechnology*, 23, 758–765.

Appendix A. MYOSIN CROSS BRIDGE REACTION RATES

The mass action rate equations for myosin cross bridge model are given as:

$$r_1 = k_1 \cdot M', \tag{A.1}$$
$$r_2 = k_2 \cdot M \cdot A, \tag{A.2}$$
$$r_3 = k_3 \cdot A\text{-}M', \tag{A.3}$$
$$r_4 = k_4 \cdot A\text{-}M \cdot ATP. \tag{A.4}$$

The used parameters are taken from Howard (2001) with $k_1 = 100$, $k_2 = 30s^{-1}$, $k_3 = 10000s^{-1}$ and $k_4 = 200s^{-1}$.